Oxovanadium(IV) and -(V) Complexes with Aminoalcohol Ligands: Synthesis, Structure, Electrochemical, and Magnetic Properties☆

Winfried Plass

Fakultät für Chemie, Universität Bielefeld,
Postfach 100131, D-33501 Bielefeld, Germany
Fax: (internat.) +49(0)521/106-6146
E-mail: winfried.plass@uni-bielefeld.de

Received December 22, 1997

Keywords: Aminoalcohol ligands / Hydrogen bonds / Magnetic properties / Oxo complexes / Vanadium

The aminoalcohol ligands diethanolamine (H_2dea) and triethanolamine (H_3tea) react with $[VO(acac)_2]$ to yield the tetranuclear oxovanadium(IV) complexes $[\{VO(dea)\}_2\{VO(acac)\}_2(\mu_2\text{-}OMe)_2]$ (**1**) and $[\{VO(Htea)\}_2\{VO(acac)\}_2(\mu_2\text{-}OMe)_2]$ (**2**). In the case of the potentially bridging aminoalcohol ligands *N,N,N′,N′*-tetrakis(2-hydroxyethyl)ethylenediamine (H_4edte) and *N,N,N′,N′*-tetrakis(2-hydroxypropyl)ethylenediamine (H_4edtp) the corresponding oxovanadium(IV) complexes could not be isolated. Instead after air oxidation the ligand supported binuclear oxovanadium(V) complexes $[\{VO(acac)\}]_2(edte)]$ (**3**) and $[\{VO(acac)\}_2(edtp)]$ (**4**) are obtained. The reaction of the ligand H_4edtp with ammonium *meta*-vanadate in methanol solution leads to the methoxy bridged binuclear oxovanadium(V) complex $[(VO)_2(edtp)(\mu_2\text{-}OMe)_2]$ (**5**). The tetranuclear oxovanadium(IV) complexes can be isolated as crystalline compounds **1**·2 MeOH and **2**·2 MeOH and have been characterized by IR, UV/Vis, and ESR spectroscopy as well as cyclic voltammetry and magnetic susceptibility measurements. Single-crystal diffraction studies reveal that the complexes **1** and **2** contain a tetranuclear $\{(VO)_4(\mu_3\text{-}OR)_2(\mu_2\text{-}OR)_4\}^{2+}$ core composed of three different types of edge-shared binuclear units, whereas the oxovanadium(V) complexes **3**, **4**, and **5** posses binuclear structures, that are either ligand supported as in the case of **3** and **4** or contain a μ_2-methoxy bridged $\{(VO)_2(\mu_2\text{-}OR)_2\}^{4+}$ core as in the case of **5**. ESR and magnetic data indicate a singlet ground state for **1**·2 MeOH and **2**·2 MeOH, although competing ferromagnetic exchange interactions are operative within the tetranuclear core structure. In the solid state compounds **1**·2 MeOH and **2**·2 MeOH hydrogen bridged supramolecular structures are found. The hydrogen bonding scheme of both compounds leads to the formation of a similar chain arrangement of the tetranuclear complexes **1** and **2**.

Introduction

The increasing interest in vanadium coordination chemistry is based on its well established biological function in the oxidations states +4 and +5, e.g. as essential element for enzymatic systems like vanadium-requiring haloperoxidases and nitrogenases and the insulin-mimetic action of vanadium compounds[1]. Related with this biological aspects the coordination chemistry of oxovanadium(IV) and -(V) complexes with aminoalcohols has found special attention[2][3][4][5]. In addition the coordination chemistry of oxovanadium(IV) complexes with aminoalcohols offers easy access to model systems for the magnetic behavior of corresponding polynuclear complexes and has already led to a magnetostructural relationship for such systems[6][7]. Similarly to the well established tris(hydroxymethyl)alkane family of ligands[8] aminoalcohols can be utilized as bridging units in the formation of higher nuclear oxovanadium(IV) complexes[9].

The present study describes a synthetic approach to oxovanadium(IV) and -(V) complexes with potentially bridging and/or chelating aminoalcohol ligands depicted in Scheme 1. Besides the structural and spectroscopic characterization of these complexes special emphasis is placed on their electrochemical and magnetic properties.

Scheme 1. Aminoalcohol ligands used in this study[a]

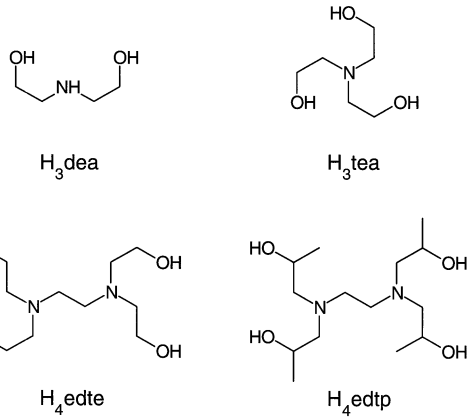

H_3dea H_3tea H_4edte H_4edtp

[a] Abbreviations: H_2dea = diethanolamine; H_3tea = triethanolamine; H_4edte = *N,N,N′,N′*-tetrakis(2-hydroxyethyl)ethylenediamine, H_4edtp = *N,N,N′,N′*-tetrakis(2-hydroxypropyl)ethylenediamine.

Results and Discussion

Syntheses

In methanol solution the aminoalcohol ligands diethanolamine (H_2dea) and triethanolamine (H_3tea) react with $[VO(acac)_2]$ (Hacac = 2,4-pentanedione) to form the neu-

  1434–1948/98/0606–0799 $ 17.50+.50/0

tral tetranuclear oxovanadium(IV) complexes [{VO(dea)}$_2$-{VO(acac)}$_2$(μ_2-OMe)$_2$] (**1**) and [{VO(Htea)}$_2${VO(acac)}$_2$-(μ_2-OMe)$_2$] (**2**). The complexes **1** and **2** are obtained as green crystalline solid materials, which are insoluble in alcohols and water but readily soluble in DMF and DMSO. Under oxygen free reaction conditions the formation of the complexes **1** and **2** is virtually independent of the ligand to [VO(acac)$_2$] ratio. However, the vanadyl ion can easily be oxidized to the +5 oxidation state in the presence of either aminoalcohol ligand. With H_3tea the air oxidation leads to the well-known oxovanadium(V) triethanolaminate[4][10]. Similar reactions with the potentially bridging aminoalcohol ligands *N,N,N′,N′*-tetrakis(2-hydroxyethyl)ethylenediamine (H_4edte) and *N,N,N′,N′*-tetrakis(2-hydroxypropyl)-ethylenediamine (H_4edtp) did not yield any isolable vanadium(IV) complexes. Nevertheless after air oxidation the ligand supported binuclear oxovanadium(V) complexes [{VO(acac)}$_2$(edte)] **3**) and [{VO(acac)}$_2$(edtp)] (**4**) can be isolated, which are isoluble in common organic solvents. For both complexes **3** and **4** only one of the acetylacetonate ligands at the vanadyl ion is replaced by the aminoalcohol ligand. Utilizing ammonium *meta*-vanadate as starting material the reaction with the ligand H_4edtp in methanol solution afforded the methoxy bridged binuclear oxovanadium(V) complex [(VO)$_2$(edtp)(μ_2-OMe)$_2$] (**5**). **5** is readily soluble in DMF and DMSO but only sparingly soluble in alcohols.

Crystal Structure Descriptions

The molecular structures of the tetranuclear complexes **1** and **2** are shown in Figures 1 and 2. In both complexes the aminoalcohols, H_2dea and H_3tea, coordinate as tridentate ligands in their dianionic form and occupy three facial positions at the vanadium center V1 leading structurally similar {VO(dea)(OMe)}$^-$ and {VO(Htea)(OMe)}$^-$ fragments. Dimers of these fragments arranged in an *anti*-coplanar configuration constitute the central units of complexes **1** and **2** with the oxygen donors O3 and O3′ in the bridging positions. The formal condensation of two {VO(acac)}$^+$ fragments onto the trigonal faces of the central fragments established by the coordinated alkoxy ligands (O3, O4′, O5 and O3′, O4, O5′) leads to the tetranuclear complexes **1** and **2**. The resulting {(VO)$_4$(μ_3-OR)$_2$(μ_2-OR)$_4$}$^{2+}$ core structure of **1** and **2** generally resembles that of an earlier reported Schiff base substituted tetranuclear oxovanadium(IV) complex[9] and corresponds to the well-known {M_4O_{16}} condensation motif found for high valent transition-metal systems[8][11]. The actual orientation pattern of the oxo groups is directed by the *trans* effect generally observed for such strong terminal ligands, i.e. all are arranged *trans* to the μ_3-bridging oxygen donors O3 and O3′. Consequently, the {(VO)$_4$(μ_3-OR)$_2$(μ_2-OR)$_4$}$^{2+}$ core of **1** and **2** consists of five edge shared binuclear arrangements: one with *anti*-coplanar (V1···V1′: 329.0(2) pm for **1**, 326.6(2) pm for **2**), two with *syn*-coplanar (V1···V2 and V1′···V2′: 342.2(2) pm for **1**, 341.9(2) pm for **2**), and two with twist configuration (V1···V2′ and V1′···V2: 329.5(2) pm for **1**, 330.8(2) pm for **2**).

Figure 1. Molecular structure **1** in crystals of **1**·2 MeOH[a]

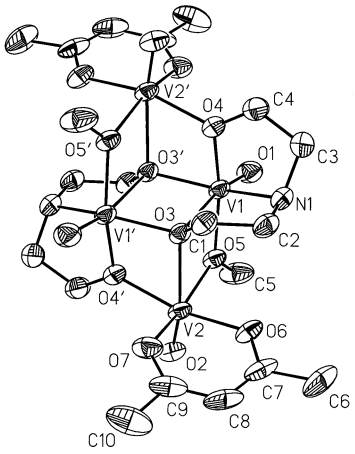

[a] The thermal ellipsoids are drawn at the 50% probability level; hydrogen atoms are omitted; atoms related by the crystallographic inversion center are denoted with a′ in the labelling scheme; selected bond lengths and metal−metal distances [pm]: C1−O1 160.5(2), V1−O3 222.1(2), V1−O3′ 201.5(2), V1−O4 195.1(2), V1−O5 201.1(2), V1−N1 215.2(3), V2−O2 159.8(2), V2−O3 235.6(2), V2−O4′ 201.0(2), V2−O5 199.1(2), V2−O6 199.9(2), V2−O7 200.2(2), V1···V2 342.2(2), V1···V2′ 329.5(2), V1···V1′ 329.0(2), V2···V2′ 585.8(3); selected bond angles [°]: O1−V1−O3 166.80(9), O2−V2−O3 164.75(9), V1−O3−V2 96.75(7), V1−O3−V1′ 101.80(8), V1′−O3−V2 97.51(8), V1−O4−V2′ 112.59(10), V1−O5−V2 117.58(9).

Figure 2. Molecular structure of **2** in crystals of **2**·2 MeOH[a]

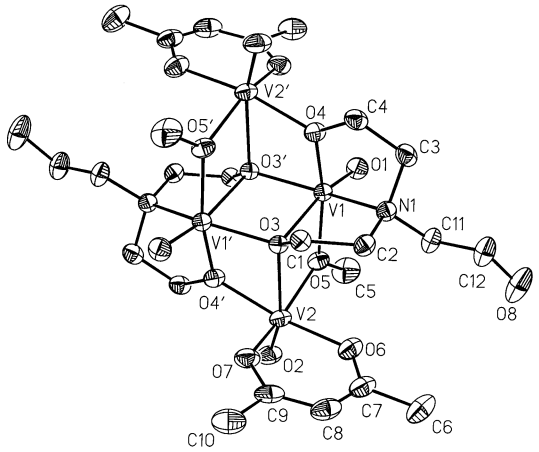

[a] The thermal ellipsoids are drawn at the 50% probability level; hydrogen atoms are omitted; atoms related by the crystallographic inversion center are denoted with a′ in the labelling scheme; selected bond lengths and metal−metal distances [pm]: V1−O1 160.8(2), V1−O3 219.8(2), V1−O3′ 201.4(2), V1−O4 193.9(2), V1−O5 203.5(2), V1−N1 217.7(3), V2−O2 159.6(2), V2−O3 237.3(2), V1−O4′ 200.4(2), V2−O5 197.5(2), V2−O6 200.8(3), V2−O7 200.1(3), V1···V2 341.9(2), V1···V2′ 330.8(2), V1···V1′ 326.6(2), V2···V2′ 588.2(2); selected bond angles [°]: O1−V1−O3 167.22(11), O2−V2−O3 163.32(11), V1−O3−V2 96.72(8), V1−O3−V1′ 101.57(9), V1′−O3−V2 97.54(9), V1−O4−V2′ 114.08(11), V1−O5−V2 116.97(11).

The crystal structures of the compounds **1**·2 MeOH and **2**·2 MeOH are characterized by the fact that both complexes contain hydrogen bond donors (**1**: NH, **2**: OH) as well as different possible acceptors. Moreover, also the additional molecules of methanol present in the crystal structures are involved in the hydrogen bonding networks. In the

hydrogen bonding scheme of **1** · 2 MeOH depicted in Figure 3 each tetranuclear oxovanadium(IV) complex takes part in the four equivalent hydrogen bonds with a N−H···O−H···O=V arrangement (N1, O1m, O1a). This leads to the formation of a hydrogen bridged chain along the [010] direction with a shortest V···V separation of 673 pm between neighboring complexes. Although the nitrogen atom of the H_3tea ligand present in **2** has lost its hydrogen donor ability due to the third substituted ethoxy group, the hydrogen bonding scheme observed for **2** · 2 MeOH depicted in Figure 4 is rather similar to that found for **1** · 2 MeOH. Nevertheless, in contrast to **1** · 2 MeOH the crystal structure of **2** · 2 MeOH exhibits two topologically different types of hydrogen bonds that can be characterized as bridging and terminal. The bridging of the oxovanadium(IV) complexes is facilitated by O−H···O=V hydrogen bonds between the dangling ethoxy groups and the oxo groups of the central binuclear unit (O8···O1a). As a result a hydrogen bridged chain along the [100] direction with a shortest V···V separation of 650 pm between neighboring complexes is formed. Whereas the methanol molecules present in **2** · 2 MeOH participate in terminal hydrogen bonds to one of the oxygen donors of the acetylacetonate ligands (O1m···O7).

Figure 3. Representation of the hydrogen bonding scheme of **1** · 2 MeOH[a]

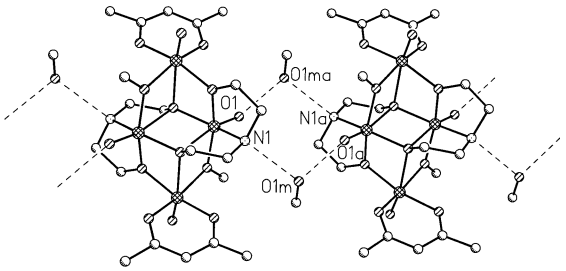

[a] Selected distances [pm]: O1−O1ma 274, N1−O1m 293.

Figure 4. Representation of the hydrogen bonding scheme of **2** · 2 MeOH[a]

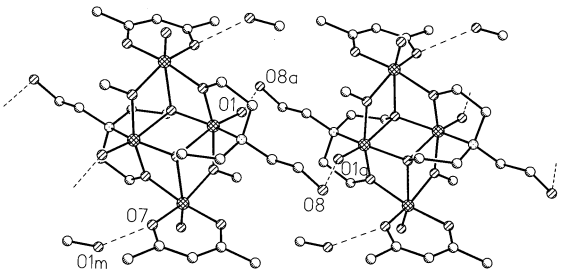

[a] The scheme is only shown for one of the enantiomeric chains; selected distances [pm]: O1−O8a 281, O1m−O7 289.

The centrosymmetric molecular structure of the ligand supported binuclear complex **3** is depicted in Figure 5. The oxovanadium(V) centers are coordinated by an acetylacetonate ligand and one of the diethanolamine fragments of the $edte^{4-}$ ligand affording an octahedral coordination environment. Basically the same molecular structure can be expected for the analogous binuclear oxovanadium(V) complex **4**, except that different stereochemical configurations are possible at the chiral carbon centers. Figure 6 shows the molecular structure derived for **4**. The observed disorder of the carbon atoms C14, C17, C20, and C23 is consistent with the occurrence of all possible stereochemical isomers in the solid state. As expected the observed bond lengths and angles for the oxovanadium(V) centers are the same for both complexes **3** and **4** within the estimated standard deviations.

Figure 5. Molecular structure of **3**[a]

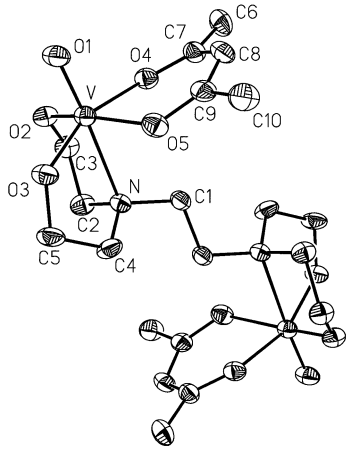

[a] The thermal ellipsoids are drawn at the 50% probability level; hydrogen atoms are omitted; selected bond lengths [pm]: V−O1 159.3(4), V−O2 181.6(4), V−O3 181.8(4), V−O4 200.5(4), V−O5 201.3(4), V−N 242.7(4); selected bond angles [°]: O1−V−O2 99.2(2), O1−V−O3 100.3(2), O1−V−O4 99.0(2), O1−V−O5 96.3(2), O1−V−N 176.6(2).

Figure 6. Molecular structure of **4**[a]

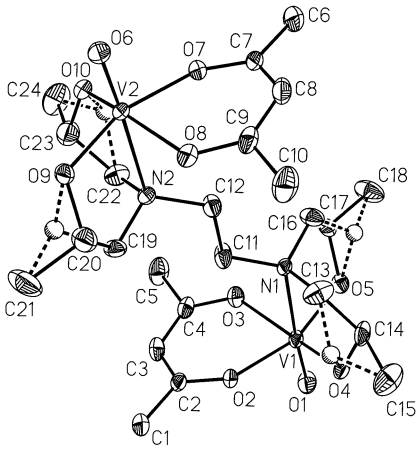

[a] The thermal ellipsoids are drawn at the 30% probability level; hydrogen atoms are omitted; C14, C17, C20, and C23 are disordered, the positions corresponding to the (*S*) configuration are represented by shaded circles and the corresponding bonds by broken lines; selected bond lengths [pm]: V1−O1 160.4(3), V1−O2 200.6(2), V1−O3 202.0(3), V1−O4 183.2(2), V1−O5 181.4(2), V1−N1 244.6(3), V2−O6 159.5(2), V2−O7 202.0(2), V2−O8 201.3(3), V2−O9 181.8(2), V2−O10 182.6(2), V2−N2 244.8(3); selected bond angles [°]: O1−V1−O2 98.76(12), O1−V1−O3 98.64(13), O1−V1−O4 99.78(13), O1−V1−O5 100.30(13), O1−V1−N1 176.43(12), O6−V2−O7 97.69(12), O6−V2−O8 98.93(13), O6−V2−O9 99.70(12), O6−V2−O10 101.31(13), O6−V2−N2 177.18(12).

The crystal structure analysis of **5** reveals the formation of a binuclear μ_2-methoxy bridged $\{(VO)_2(\mu_2\text{-}OR)_2\}^{4+}$ core

(see Figure 7). The coordination of the hexadentate aminoalcohol ligand edtp^{4-} leads to an octahedral coordination environment for both oxovanadium(V) centers. In contrast to **4** the crystal structure of **5** is consistent with the presence of just one diastereomer derived from the enantiomeric ligand pair (*R,R,R,R*)-H_4edtp and (*S,S,S,S*)-H_4edtp. In Figure 7 only the molecular structure of [$(VO)_2$\{(*S,S,S,S*)-edtp\}(μ_2-OMe)$_2$] is depicted, which is related to the enantiomeric structure of [$(VO)_2$\{(*R,R,R,R*)-edtp\}(μ_2-OMe)$_2$] by an crystallographic mirror plane (with V1, V2, O1, O2, and N1 lying on the mirror plane). Although not enforced by a crystallographic symmetry element the molecular structure of **5** is consistent with an approximate C_2 symmetry with the twofold axis perpendicular to the mean plane given by V1, O3, V2, and O3a ($\Sigma \measuredangle$ = 355°).

Figure 7. Molecular structure of **5**[a]

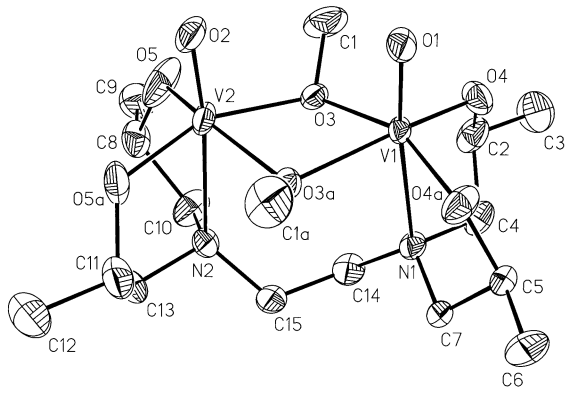

[a] The thermal ellipsoids are drawn at the 30% probability level; hydrogen atoms are omitted; atoms related by the crystallographic mirror plane are denoted with the suffix a in the labelling scheme; for the carbon and nitrogen atoms only the positions corresponding to the all (*S*) form of the edtp^{4-} ligand are shown; selected bond lengths [pm]: V1−O1 159.5(2), V1−O3 200.14(14), V1−O4 181.1(2), V1−N1 240.3(2), V2−O2 160.0(2), V2−O3 199.8(2), V2−O5 181.1(2), V2−N2 241.7(4); selected bond angles [°]: O1−V1−O3 99.60(8), O1−V1−O4 98.15(7), O1−V1−N1 173.75(1), O3−V1−O4 90.00(8), O3−V1−O3a 72.33(8), O3−V1−O4a 156.75(8), O2−V2−O3 99.70(8), O2−V2−O5 98.86(2), O2−V2−N2 170.93(12), O3−V2−O5 90.14(9), O3−V2−O3a 72.46(8), O3−V2−O5 90.14(9), V1−O3−V2 105.22(7).

Spectroscopic and Electrochemical Characterization

The IR spectra of the tetranuclear complexes **1** and **2** are consistent with their centrosymmetric core structure and the presence of vanadyl acetylacetonate fragments. The bands related with the V=O stretching vibrations are observed at 950 and 975 cm^{-1}, with the latter being characteristic for an octahedral coordinated vanadyl acetylacetonate fragment[6][9]. Although the complexes **3** and **4** contain an oxidized oxovanadium(V) group, their band related with the V=O stretching vibration is observed at a similar value of about 970 cm^{-1}. For **1** · 2 MeOH and **2** · 2 MeOH the observed IR bands due to their O−H and N−H stretching vibrations are in accord with their hydrogen bridged supramolecular structure found in the solid state (cf. Figures 3 and 4).

The NMR spectra recorded for **5** are consistent with the presence of only one diastereomer with C_2 symmetry in solution. According to the results of the crystallographic analysis this corresponds to the enantiomeric pair [$(VO)_2$\{(*S,S,S,S*)-edtp\}(μ_2-OMe)$_2$] and [$(VO)_2$\{(*R,R,R,R*)-edtp\}(μ_2-OMe)$_2$]. Consequently the protons of the methylene groups are diastereotopic. The observed coordination induced shifts of the ^{1}H and ^{13}C resonances (see Experimental Section) toward lower fields are consistent with the structure of the chelate rings and generally an intact molecular structure of **5** in solution[2][4][5][12].

To probe the electrochemical properties of the tetranuclear oxovanadium(IV) complexes **1** and **2** cyclic voltammetry measurements have been performed. Figure 8 shows representative cyclic voltammograms of a solution of **2** · MeOH in DMF measured at a gold working electrode. As expected the neutral oxovanadium(IV) complexes **1** and **2** can be oxidized. Figure 8 shows that four oxidation half waves can be observed in the cyclic voltammogram (A, B, C, and D). The first oxidative peak at E_a = 0.47 V (A) possesses a reductive counterpart at E_c = 0.37 V (G). Based on the scan rate dependence of the peak separation and the peak current ratio ($i_a/i_c \approx 1$) the wave given by A/G is found to be quasi-reversible. On the contrary, for the oxidative peaks B (E_a = 0.73 V) and C (E_a = 0.90 V) no related reduction half waves are observed as can be seen from the cyclic voltammogram measured with an anodic potential limit of about 1.0 V (see broken line in Figure 8). Upon scanning through the fourth oxidation half wave D (E_a = 1.17 V) two new reduction half waves E (E_c = 1.01 V) and F (E_c = 0.61 V) are observed. The reduction half waves E and F can be assigned to a new species derived by a chemical reaction of the positively charged complex after the last oxidation step D. This is further evidenced by the observed scan rate dependence of the two reduction half waves E and F.

Figure 8. Cyclic voltammograms of **2**[a]

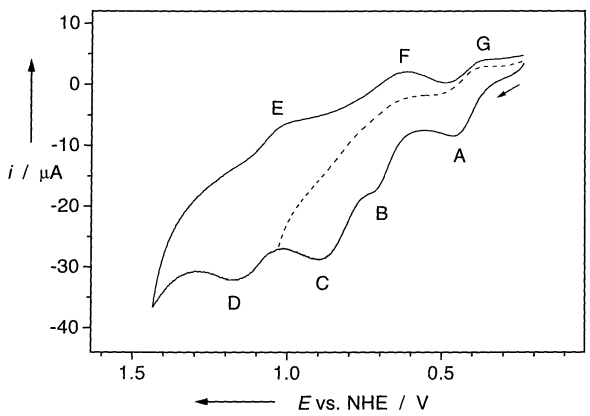

[a] Solvent DMF; tetra-*n*-buthylammonium perchlorate is used as supporting electrolyte at 0.1 M concentration and the concentration of the compound **2**·2 MeOH is about 1 mM; scan rate 50 mV/s; the broken line represents a scan with an anodic reversion potential of about 1.0 V; A, B, C, and D represent anodic peak potentials and E, F, and G stand for cathodic peak potentials (see text).

ESR Spectra and Magnetic Properties of 1 and 2

The X-band ESR powder spectra of **1** · 2 MeOH and **2** · 2 MeOH recorded at room temperature show a broad unstructured band at $g = 1.97$ and a second weak resonance at half-field, indicating the spectra are the result of exchange coupled spin systems[13]. The temperature dependence of the spectra indicates singlet ground states for **1** and **2**. At very low temperatures only the resonance signal of a residual monomeric oxovanadium(IV) impurity can be detected.

The magnetic susceptibility data of polycrystalline samples of **1** · 2 MeOH and **2** · 2 MeOH were measured in a temperature range from 4 to 280 K. The temperature dependence of the molar magnetic susceptibility χ_M in both cases goes through a maximum which is indicative for antiferromagnetic exchange interactions to be operative. At low temperatures χ_M is increasing again due to the presence of paramagnetic impurities. The $\chi_M T$ values at low temperatures are in accord with an $S = 0$ ground state of **1** and **2**, as suggested by the ESR spectra.

The observed ESR spectra and magnetic properties of **1** · 2 MeOH and **2** · 2 MeOH resemble those observed for an earlier reported oxovanadium(IV) complex with the same tetranuclear core structure[9]. On the basis of a general magneto-structural relationship for edge-shared binuclear oxovanadium(IV) units[6], both antiferro- and ferromagnetic interactions can be expected to be operative within the $\{(VO)_4(\mu_3\text{-}OR)_2(\mu_2\text{-}OR)_4\}^{2+}$ core of **1** and **2**. The spin topology and the notation of the magnetic exchange interaction parameters are depicted in Scheme 2. As a consequence of the given spin topology the expected antiferro- (J_{sc}) and ferromagnetic exchange interactions (J_{ac} and J_t) cannot be simultaneously satisfied.

Scheme 2. Spin topology of the $\{(VO)_4(\mu_3\text{-}OR)_2(\mu_2\text{-}OR)_4\}^{2+}$ core[a]

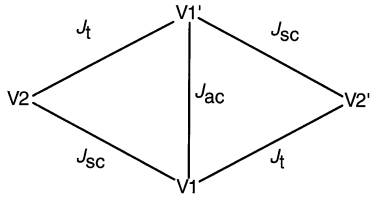

[a] The magnetic exchange coupling constants are denoted as follows: J_{ac} for *anti*-coplanar, J_{sc} for *syn*-coplanar, and J_t for twist configurations.

Based on data observed for other complexes with similar configurations of the binuclear oxovanadium(IV) units[6][9], the relative ratio of the exchange interaction parameters can be estimated as $-J_{sc} \gg J_{ac} \approx J_t$. Although competing magnetic interactions are operative within the tetranuclear core, a simplified binuclear model proved to be sufficient to describe the magnetic data of such a tetranuclear core structure with the given estimated parameter ratio[9]. This model refers to the picture that both pairs with *syn*-coplanar configuration (V1···V2 and V1′···V2′) should be predominantly coupled to form two virtually independent $S=0$ ground states. A quantitative analysis of the magnetic data has been performed using the Heisenberg−Dirac-van Vleck Hamiltonian given in Eq. 1.

$$\hat{\mathbf{H}} = -J(\hat{\mathbf{S}}_1 \cdot \hat{\mathbf{S}}_2 + \hat{\mathbf{S}}_{1'} \cdot \hat{\mathbf{S}}_{2'}) \quad (1)$$

Although only one exchange interaction constant is used in the analytical expression, reasonably good fits to the experimental data of **1** · 2 MeOH and **1** · 2 MeOH can be achieved. The magnetic parameters derived for the simplified isotropic spin Hamiltonian according to Eq. 1 are $g = 1.89$ and $J = -165$ cm^{-1} for **1** · 2 MeOH and $g = 1.94$ and $J = -171$ cm^{-1} for **2** · 2 MeOH. The rather strong antiferromagnetic coupling constants observed for both complexes are in good agreement with the data reported for other complexes containing binuclear units with *syn*-coplanar configuration (V···V 333 pm, $J = -334$ cm^{-1}[14] and V···V 341 pm, $J = -152$ cm^{-1}[9]) and can be explained on the basis of the possible superexchange mechanism through the bridging methoxy oxygen donors (O5 and O5′).

This work was supported by the *Deutsche Forschungsgemeinschaft*, the *Fonds der Chemischen Industrie*, and the *Herbert Quandt-Stiftung der VARTA AG.*

Experimental Section

NMR: ^{1}H, ^{13}C, ^{51}V, ^{1}H-^{1}H COSY, ^{1}H-^{13}C COSY, and ^{1}H-^{1}H NOESY NMR spectra were recorded on a Bruker DRX500 (^{1}H 500 MHz, ^{13}C 125.8 MHz, ^{51}V 131.5 MHz) spectrometer. Chemical shifts δ are reported with reference to external tetramethylsilan (^{1}H and ^{13}C) and $VOCl_3$ (^{51}V). − IR: Solid samples were measured either as KBr pellets or Nujol mulls between CsI plates using a Bruker IFS66 FT-IR spectrometer. − Raman: Solid samples were measured as powder on aluminium support using a Bruker IFS66/FRA106 (λ_e = 1064 nm) spectrometer. − UV/Vis: Spectra were recorded on Beckman Acta MIV (solid state reflection, cellulose as calibration standard) and Schimadzu UV-160A spectrometers (solution transmission). − Cyclic voltammetry: Princeton Applied Research VersaStat (Model 253). Cyclic voltammograms have been measured at room temperature with a three-electrode system composed of a gold working electrode, a platinum auxiliary electrode, and a platinum wire as reference electrode. The surface of the the gold working electrode was polished before each measurement. The reported potentials were referenced compared to the potential of the ferrocenium/ferrocene couple [$E^0(Fc^+/Fc) = 400$ mV vs. NHE] as internal standard[15]. The solvent DMF was dried and saturated with argon. Tetra-*n*-buthylammonium perchlorate was used as the supporting electrolyte at 0.1 M concentration and the solutions of the complexes were about 1 mM in concentration. − Powder diffraction: Powder diffraction diagrams were measured of solid samples on Al support with a Philips PW3710 powder diffractometer using Cu-$K\alpha$ radiation. − ESR: X-Band ESR spectra were recorded using a Bruker ECS106 spectrometer at a microwave frequencies of 9.48 GHz with 2,2-diphenyl-1-picrylhydrazyl as standard. − Magnetic susceptibility: Magnetic susceptibility measurements from 4 to 280 K were performed by using a Quantum Design MPMS2 SQUID magnetometer. All data were collected at an applied field of 10 kOe. The diamagnetic corrections were estimated from Pascal's constants. The susceptibility data were further corrected for temperature-independent paramagnetism (TIP) and the presence of paramagnetic impurity. For details see ref.[9]. − Melting points (uncorrected): Electrothermal melting point apparatus. − Elemental analyses: LECO CHNS-932 Analyzer.

Preparation of [{VO(dea)}$_2${VO(acac)}$_2$(μ_2-OMe)$_2$] · 2 MeOH (**1** · 2 MeOH) *and [{VO(Htea)}$_2${VO(acac)}$_2$(μ_2-OMe)$_2$] · 2 MeOH* (**2** · 2 MeOH): All manipulations were carried out under an argon atmosphere using Schlenk line techniques. The solvent methanol was purified and dried using standard methods. The ligand (9.5 mmol, i.e. 1.00 g of H_2dea or 1.42 g of H_3tea) dissolved in 5 ml methanol was added to a solution of 2.54 g (9.5 mmol) [VO(acac)$_2$] in 20 ml methanol. The resulting green solution was heated at reflux for 2 h and subsequently allowed to stand at room temperature. Within 3−4 days green crystals began to grow. After an additional week the crystalline compounds were isolated by filtration and washed with methanol. A second crop of material was obtained from the filtrate after removing solvent to about 1/3 of the original volume. The isolated solid materials can be handled in air. Within about 8 weeks the crystals start to decompose due to the loss of cocrystallized methanol.

1 · 2 MeOH: Yield 0.98 g (52%), dec. 165°C. − $C_{22}H_{46}N_2O_{16}V_4$ (798.4): calcd. C 33.10, H 5.81, N 3.51, found: C 33.31, H 5.69, N 3.68. − Selected IR data (Nujol mull between CsI plates, cm^{-1}): ν(OH) 3370 br. w, ν(NH) 3240 m, ν(C⩵C) + ν(C⩵O) 1583 vs and 1518 vs, ν(V=O) 978 vs (V2 cf. Figure 1), ν(V=O) 950 vs (V1 cf. Figure 1). − UV/Vis [DMF, $\tilde{\nu}_{max}$ in 10^3 cm^{-1} (ε in lmol^{-1} cm^{-1})]: 22.4 (23, sh), 16.0 (55), 11.5 (110). − UV/Vis (solid state, reflectance, $\tilde{\nu}_{max}$ in 10^3 cm^{-1}): 31.8, 26.7 (sh), 22.5 (sh), 16.2, 11.2.

2 · 2 MeOH: Yield 1.59 g (76%), dec. 159°C. − $C_{26}H_{54}N_2O_{18}V_4$ (886.5): calcd. C 35.23, H 6.14, N 3.16, found: C 35.01, H 5.82, N 3.11. − Selected IR data (Nujol mull between CsI plates, cm^{-1}): ν(OH) 3515 w, ν(OH) 3410 m, ν(C⩵C) + ν(C⩵O) 1582 vs and 1521 vs, ν(V=O) 973 vs (V2 cf. Figure 2), ν(V=O) 954 vs (V1 cf. Figure 2). − UV/Vis [DMF, $\tilde{\nu}_{max}$ in 10^3 cm^{-1} (ε in lmol^{-1} cm^{-1})]: 22.3 (20, sh), 16.1 (54), 11.7 (103). − UV/Vis (solid state, reflectance, $\tilde{\nu}_{max}$ in 10^3 cm^{-1}): 31.6, 26.3 (sh), 22.2 (sh), 16.4, 11.4.

Preparation of [{VO(acac)}$_2$(edte)] (**3**) *and [{VO(acac)}$_2$(edtp)]* (**4**): The ligand (7.5 mmol, i.e. 1.78 g of H_4edte or 2.19 g of H_4edtp, the latter being a mixture of all possible diastereomers) dissolved in 5 ml methanol was added to a solution of 4.00 g (15 mmol) [VO(acac)$_2$] in 40 ml methanol. At room temperature a slow stream of air was bubbled through the stirred green solution (for about 2 h). The resulting brown solution was kept at room temperature for crystallization. Orange needles began to grow after about 1 day and after additional 2 days the crystalline compound was isolated by filtration and washed with methanol. A second crop of material was obtained from the filtrate after reducing the solution volume to about 20 ml.

3: Yield 2.51 g (59%), dec. 148°C. − $C_{20}H_{34}N_2O_{10}V_2$ (564.4): calcd. C 42.56, H 6.07, N 4.96; found: C 42.37, H 6.28, N 4.68. − Selected IR data (Nujol mull between CsI plates, cm^{-1}): ν(C⩵C) + ν(C⩵O) 1574 s and 1527 s, ν(V=O) 970 vs. − Selected Raman data (powder on Al support, λ_e = 1064 nm, 35 mW, cm^{-1}): ν(V=O) 964 s.

4: Yield 2.32 g (50%), dec. 136°C. − $C_{24}H_{42}N_2O_{10}V_2$ (620.5): calcd. C 46.46, H 6.82, N 4.51; found: C 46.27, H 6.68, N 4.66. − Selected IR data (Nujol mull between CsI plates, cm^{-1}): ν(C⩵C) + ν(C⩵O) 1576 vs and 1531 vs, ν(V=O) 972 vs. − Selected Raman data (powder on Al support, λ_e = 1064 nm, 90 mW, cm^{-1}): ν(V=O) 969 s.

Preparation of [(VO)$_2$(edtp)(μ_2-OMe)$_2$] (**5**): NH_4VO_3 (2.8 g, 24 mmol) was added to a solution of H_4edtp (3.50 g, 12 mmol) in 50 ml methanol containing all possible diastereomers of the ligand. The resulting mixture was heated at reflux for 8 h. The hot reaction mixture was filtered to remove unreacted NH_4VO_3. Upon cooling the filtrate to room temperature orange crystals of **5** · *x* MeOH formed. The number of methanol molecules present in the crystalline material is estimated to x = 0.3 based on the elemental analysis and NMR data and is consistent with the crystal structure data.

5: Yield 0.38 g (6%), dec. 169°C. − $C_{16}H_{34}N_2O_8V_2$ · 0.3 MeOH (493.9): calcd. C 39.64, H 7.18, N 5.67; found: C 39.66, H 7.36, N 5.74. − Selected IR data (Nujol mull between CsI plates, cm^{-1}): ν(V=O) 963 vs. − Selected Raman data (powder on Al support, λ_e = 1064 nm, 150 mW, cm^{-1}): ν(V=O) 961 m. − ^{1}H NMR (500 MHz, [D$_6$]DMSO): δ = 1.00 (d, ^3J = 6.0 Hz, 6H, CH_3), 1.18 (d, ^3J = 6.0 Hz, 6H, CH_3), 2.23−2.31 [m; 6H, CH_2NCH_2CH(CH$_3$)OV], 2.62−2.67 (m, 2H, NCH_2CH(CH$_3$)OV), 2.80−2.85 [m, 2H, NCH_2CH(CH$_3$)OV], 3.23−3.31 (m, 2H, CH_2N), 4.21 (s, 6H, OCH_3), 4.70 (m, 2H, NCH$_2$CH(CH$_3$)OV], 4.81 (m, 2H, NCH$_2$CH(CH$_3$)OV). − ^{13}C NMR (125.8 MHz, [D$_6$]DMSO): δ = 19.7 (CH_3), 21.4 (CH_3), 51.6 (CH_2N), 59.7 [NCH_2CH(CH$_3$)OV], 63.7 [NCH_2CH(CH$_3$)OV], 67.5 (OCH_3), 76.3 [CH_2CH(CH$_3$)OV], 78.2 [CH_2CH(CH$_3$)OV]. − ^{51}V NMR (131.5 MHz, [D$_6$]DMSO): δ = −444.

Crystal Structure Determinations of **1** · 2 MeOH, **2** · 2 MeOH *and* **3**: The crystallographic data of **1** · 2 MeOH, **2** · 2 MeOH, and **3** were collected with ω-scan technique on a Siemens R3m/V diffractometer using graphite monochromated Mo-$K\alpha$ (λ = 71.073 pm) radiation. The unit cell parameters were obtained by least-squares refinement of the angular settings from well centered reflections in the 2Θ range of 18−30°. Lorentz and polarization corrections as well as an absorption correction based on azimuthal ψ scans were applied to the diffraction data. The structures were solved by direct methods (SHELXTL)[16] and subsequent full-matrix least-squares refinement of the function $\Sigma w(F_o^2 - F_c^2)^2$ $\{w = 1/[\sigma^2(F_o^2) + (A \cdot P)^2 + B \cdot P]$ with $P = (F_o^2 + 2F_c^2)/3\}$[17]. All non-hydrogen atoms were refined with anisotropic displacement parameters. The hydrogen atoms were treated using the riding model with their isotropic displacement parameters fixed at 1.2 times the value of the non-hydrogen atom attached. For the hydrogen atoms of the methyl as well as hydroxyl groups their conformation was additionally fitted to the difference Fourier map.

1 · 2 MeOH: $C_{22}H_{46}N_2O_{16}V_4$; formula weight 798.4; crystal size 0.5 × 0.5 × 0.4 mm; triclinic space group $P\bar{1}$ (No. 2); T = 188 K;; a = 773.5(3), b = 998.7(3), c = 1241.6(4) pm, α = 103.10(2), β = 107.69(2), γ = 106.13(2)°; V = 0.8255(5) nm^3; Z = 1; $\rho_{calcd.}$ = 1.606 g/cm^3; μ(Mo-K_α) = 1.168 mm^{-1}; 2Θ range 4−54°; 3553 independent reflections ($R_{int.}$ = 0.022); 204 parameters; A = 0.08, B = 0.5; $wR2$ = 0.137; $R1$ = 0.047 for 3064 reflections with $F > 4\sigma(F)$; max./min. residual electron density in the final difference Fourier map 0.9/−0.6 · 10^{-6} e/pm^3.

2 · 2 MeOH: $C_{26}H_{54}N_2O_{18}V_4$; formula weight 886.5; crystal size 0.3 × 0.2 × 0.2 mm; monoclinic space group $P2_1/c$ (No. 14); T = 188 K; a = 965.4(2), b = 1677.0(4), c = 1677.0(4) pm, β = 104.65(2)°; V = 1.8622(8) nm^3; Z = 2; $\rho_{calcd.}$ = 1.581 g/cm^3; μ(Mo-K_α) = 1.048 mm^{-1}; 2Θ range 4−54°; 4095 independent reflections ($R_{int.}$ = 0.020); 232 parameters; A = 0.05, B = 2.7; $wR2$ = 0.122; $R1$ = 0.046 for 3028 reflections with $F > 4\sigma(F)$; max./min. residual electron density in the final difference Fourier map 0.5/−0.5 · 10^{-6} e/pm^3.

3: $C_{20}H_{34}N_2O_{10}V_2$; formula weight 564.4; crystal size 0.25 × 0.15 × 0.05 mm; monoclinic space group $P2_1/n$ (No. 14); T = 188 K; a = 812.2(3), b = 1165.2(5), c = 1298.3(6) pm, β = 102.65(3)°; V = 1.1989(9) nm^3; Z = 2; $\rho_{calcd.}$ = 1.563 g/cm^3; μ(Mo-K_α) = 0.837 mm^{-1}; 2Θ range 4−54°; 2632 independent reflections ($R_{int.}$ = 0.030); 156 parameters; A = 0.07, B = 2.5; $wR2$ = 0.176; $R1$ = 0.067 for 1675 reflections with $F > 4\sigma(F)$; max./min. residual electron density in the final difference Fourier map 0.6/−0.4 · 10^{-6} e/pm^3.

Crystal Structure Determinations of **4** *and* **5**: The crystallographic data of **4** and **5** were collected on a Siemens SMART-CCD diffractometer (ω-scans with 0.3° per frame) using graphite monochromated Mo-$K\alpha$ (λ = 71.073 pm) radiation. The intensities of the reflections of a hemisphere have been measured (SMART). Lorentz and polarization corrections as well as an empirical absorption correction based on the intensities of equivalent reflections measured at different angular settings have been performed (SAINT and SADABS). The structure was solved by direct methods (SHELXTL)[16] and subsequent full-matrix least-squares refinement of the function $\Sigma w(F_o^2 - F_c^2)^2$ $\{w = 1/[\sigma^2(F_o^2) + (A \cdot P)^2 + B \cdot P]$ with $P = (F_o^2 + 2F_c^2)/3\}$[17]. All non-hydrogen atoms were refined with anisotropic displacement parameters. The hydrogen atoms were treated using the riding model with their isotropic displacement parameters fixed at 1.2 times the value of the non-hydrogen atom attached. For the hydrogen atoms of the methyl as well as hydroxyl groups their conformation was additionally fitted to the difference Fourier map.

For **4** the observed systematic absences suggest either of the orthorhombic space groups $Pca2_1$ and *Pbcm*. Attempts to solve the structure in the centrosymmetric space group *Pbcm* were unsuccessful. This led in agreement with intensity statistics to the noncentrosymmetric orthorhombic space group $Pca2_1$ as final choice. The refinement afforded a Flack parameter[18] of about 0.4, which could not be reduced upon inversion of the parameter set. Therefore the final structure refinement was performed assuming racemic twinning, which led to a refined Flack parameter of 0.42(2). Also the refinement in the chiral subgroup $P2_1$ was attempted but did not give any evidence for the presence of any particular chiral molecular structure. The presence of all possible diastereomers is consistent with the observed disorder of the chiral carbon atoms of the edtp^{4-} ligand (C14, C17, C20, and C23) on two positions corresponding to their respective (*R*) and (*S*) configurations (in Figure 6 only the positions for the (*R*) configurations are represented as ellipsoids).

The additional methanol molecule present in **5** is highly disordered and only the respective oxygen atom could be located from the difference Fourier map and refined with an isotropic displacement parameter.

4: $C_{24}H_{42}N_2O_{10}V_2$; formula weight 620.5; crystal size 0.4 × 0.4 × 0.4 mm; orthorhombic space group $Pca2_1$ (No. 29); T = 183 K; a = 2553.18(4), b = 823.11(1), c = 1396.16(1) pm; V = 2.93410(6) nm^3; Z = 4; $\rho_{calcd.}$ = 1.405 g/cm^3; μ(Mo-K_α) = 0.691 mm^{-1}; 2Θ range 4−54°; 5897 independent reflections ($R_{int.}$ = 0.027); 3298 reflections for Friedel opposites merged; 379 parameters; A = 0.06, B = 2.1; $wR2$ = 0.109; $R1$ = 0.039 for 5331 reflections with $F > 4\sigma(F)$; Flack parameter x = 0.42(2); max./min. residual electron density in the final difference Fourier map 0.5/−0.6 · 10^{-6} e/pm^3.

5: $C_{16}H_{34}N_2O_8V_2 \cdot 0.3$ MeOH; formula weight 493.9; crystal size 0.4 × 0.4 × 0.06 mm; orthorhombic space group *Pbcm* (No. 57); T = 183 K; a = 903.85(1), b = 1453.37(2), c = 1757.92(3) pm; V = 2.30925(6) nm^3; Z = 4; $\rho_{calcd.}$ = 1.421 g/cm^3; μ(Mo-M_α) = 0.852 mm^{-1}; 2Θ range 4−54°; 2593 independent reflections ($R_{int.}$ = 0.028); 208 parameters; A = 0.04, B = 1.8; $wR2$ = 0.097; $R1$ = 0.038 for 2204 reflections with $F > 4\sigma(F)$; max./min. residual electron density in the final difference Fourier map 0.5/−0.4 · 10^{-6} e/pm^3.

Further details of the crystal structure investigations may be obtained from the Fachinformationszentrum Karlsruhe; D-76344 Eggenstein-Leopoldshafen (Germany), on quoting the depository numbers CSD-408105 (**1** · 2 MeOH), CSD-408106 (**2** · 2 MeOH); CSD-408107 (**3**), CSD-408108 (**4**), and CSD-408109 (**5**).

☆ Dedicated to Professor *Achim Müller* on the occasion of his 60th birthday.

[1] [1a] H. Sigel, A. Sigel (Eds.), *Metal Ions in Biological Systems,* vol. 31: *Vanadium and Its Role in Life*, Marcel Dekker, New York, **1995**. – [1b] N. D. Chasteen (Ed.), *Vanadium in Biological Systems*, Kluwer Academic Publishers, Dordrecht, **1990**. – [1c] R. Wever, K. Kustin, *Adv. Inorg. Chem.* **1990**, *35*, 81−115.

[2] [2a] W. Plass, *Z. Anorg. Allg. Chem.* **1997**, *623*, 461−477. – [2b] W. Plass, *Inorg. Chim. Acta* **1996**, *244*, 221−227. – [2c] W. Plass, *Z. Anorg. Allg. Chem.* **1994**, *620*, 1635−1644.

[3] [3a] D. C. Crans, A. D. Keramidas, S. S. Amin, O. P. Anderson, S. M. Miller, *J. Chem. Soc. Dalton Trans.* **1997**, 2799−2812. – [3b] D. C. Crans, P. M. Ehde, P. K. Shin, L. Pettersson, *J. Am. Chem. Soc.* **1991**, *113*, 3728−3736. – [3c] D. C. Crans, R. L. Bunch, L. A. Theisen, *J. Am. Chem. Soc.* **1989**, *111*, 7597−7607. – [3d] D. C. Crans, P. K. Shin, *Inorg. Chem.* **1988**, *27*, 1797−1806. – [3e] G. J. Colpas, B. J. Hamstra, J. W. Kampf, V. L. Pecoraro, *Inorg. Chem.* **1994**, *33*, 4669−4675. – [3f] C. R. Cornman, G. J. Colpas, J. D. Hoeschele, J. Kampf, V. L. Pecoraro, *J. Am. Chem. Soc.* **1992**, *114*, 9925−9933.

[4] D. C. Crans, H. Chen, O. P. Anderson, M. M. Miller, *J. Am. Chem. Soc.* **1993**, *115*, 6769−6776.

[5] D. C. Crans, K. P. Shin, *J. Am. Chem. Soc.* **1994**, *116*, 1305−1315.

[6] W. Plass, *Angew. Chem.* **1996**, *108*, 699−703; *Angew. Chem. Int. Ed. Engl.* **1996**, *35*, 627−631.

[7] W. Plass, *Z. Anorg. Allg. Chem.* **1997**, *623*, 1290−1298.

[8] M. I. Khan, J. Zubieta in *Progress in Inorganic Chemistry* (Ed.: K. D. Karlin), Wiley-Interscience, New York, **1995**, vol. 43, pp. 1−149.

[9] W. Plass, *Inorg. Chem.* **1997**, *36*, 2200−2205.

[10] [10a] M. G. Voronkov, A. F. Lapsin, U.S.S.R. Patent 187,793 and 187,792 **1966** [*Chem. Abstr.* **1967**, *67*, 4452e, 4453f]. – [10b] R. K. Mittal, *Z. Anorg. Allg. Chem.* **1967**, *351*, 309−312.

[11] [11a] M. Mikuriya, T. Kotera, F. Adachi, S. Bandow, *Chem. Lett.* **1993**, 945−948. – [11b] I. Cavaco, J. C. Pessoa, M. T. Duarte, P. M. Matias, R. T. Henriques, *Polyhedron* **1993**, *12*, 1231−1237.

[12] M. M. Caldeira, M. L. Ramos, N. C. Oliveira, V. M. S. Gil, *Can. J. Chem.* **1987**, *65*, 2434−2440.

[13] A. Bencini, D. Gatteschi, *Electron Paramagnetic Resonance of Exchange Coupled Systems*, Springer, Berlin, **1990**.

[14] M. I. Khan, Y.-D. Chang, Q. Chen, J. Salta, Y.-S. Lee, C. J. O'Connor, J. Zubieta, *Inorg. Chem.* **1994**, *33*, 6340−6350.

[15] R. R. Gagné, C. A. Koval, G. C. Lisensky, *Inorg. Chem.* **1980**, *19*, 2854−2855.

[16] *SHELXTL,* Siemens Analytical X-Ray Instruments Inc., Madison, Wisconsin, USA, **1994**.

[17] G. M. Sheldrick, *SHELXL-93*, Universität Göttingen, **1993**.

[18] [18a] H. D. Flack, *Acta Crystallogr.* **1983**, *A39*, 876−881. – [18b] G. Bernardinelli, H. D. Flack, *Acta Crystallogr.* **1985**, *A41*, 500−511.

[97314]